文章编号：0258-7025(2010)05-1192-06

Theoretical Study of Tunable Mid-Infrared Radiation Based on Sum-Frequency Generation in Nonresonant Fresnel Phase Matching ZnSe and GaP Crystal

Zhuo Wang (王 卓) Yuye Wang (王与烨) Jianquan Yao (姚建铨)

(*College of Precision Instrument and Optoelectronics Engineering, Institute of Laser and Optoelectronics, Tianjin University, Tianjin* 300072, *China*)

Corresponding author: *annawangz@yahoo.com.cn*

Received July 1, 2009

Abstract Based on the theory of nonresonant Fresnel phase matching (FPM), tuning characteristics of second-harmonic generation (SHG) wave, the full-width at half-maximum (FWHM) acceptance bandwidth for total internal reflection angle, and the effective nonlinear coefficient of sum-frequency generation in ZnSe and GaP crystals are calculated under different polarization configurations. In theoretical calculation, the parameters, which have been reported to generate the tunable infrared waves by SHG in experiments, are adopted. The optimal quasi-phase-match conditions in ZnSe and GaP are summarized by comparing the simulated results, respectively. The calculated results show a sound theoretical basis for using FPM method to generate tunable mid-infrared wave in isotropic crystals.

Key words nonlinear optics; nonresonant Fresnel phase match; second-harmonic generation; ZnSe crystal; GaP crystal

CLCN: TN253 **Document Code**: A **doi**: 10.3788/CJL20103705.1192

1 Introduction

For decades, many interesting materials have been used in second-harmonic generation (SHG) mid-infrared radiation[1~8], such as $HgGa_2S_4$[2], $AgGaSe_2$[3], GaSe[4], and zinc-blende semiconductors (e.g., GaAs[5], ZnTe[6], GaP[7], ZnSe[8]). Among them, ZnSe crystal with a noncentrosymmetric structure attracts particular interest owing to its well understood optoelectronic properties and large nonlinear coefficient[9]. GaP crystal also has a number of attractive features that make it eminently suite for this study. It shows appreciate dispersion in visible and infrared range[10]. Its infrared active phonon-polariton is Raman active[11], allowing for SHG. However, owing to their optically isotropic characteristics, the birefringence match scenario is impossible in ZnSe and GaP crystals, and the noncollinear phase match geometry usually has to be used[12]. Because the reported experimental result has shown that the conversion efficient of the collinear geometry is much higher than that of the noncollinear geometry[13], the Fresnel phase matching (FPM) scenario as an alternative solution has been proposed to get effective conversion with co-propagating geometry.

The FPM[14] was proposed by Armstrong *et al.* firstly in 1962, who suggested to make use of the different total internal reflection phase shifts, i.e. Fresnel phase shift, in a plane-parallel plate to obtain quasi-phase-match (QPM)[14]. The FPM by total internal reflection can solve the problems of limited coherent length and low conversion efficiency of frequency upconversion in isotropic crystals. Compared with the traditional QPM condition, the processing difficulty of the multiple-bonded and orientation-patterned isotropic plates also can be solved. Nowadays, the factors[15] of Fresnel phase match scenario, such as Goos-Hanchen shift and surface roughness, which limit coherent length and output signal intensity, have been investigated in theories and in experiments[15]. We also wonder the tuning characteristics of generated SHG mid-infrared radiation and angular acceptance of SHG in FPM isotropic crystals. However, there are few related theoretical studies reported.

In this paper, based on the theory of nonresonant FPM, we calculate and analyze the tuning characteristics of SHG wave, the full-width at half-maximum (FWHM) acceptance bandwidth for the total internal reflection angle, and the effective nonlinear coefficient of sum-frequency generation in ZnSe and GaP crystals

This work was supported by the National "973" Program of China under Grant No. 2007CB10403.

under different polarization configurations. The calculated results provide a sound theoretical basis for using FPM method to generate tunable infrared wave in isotropic crystals.

2　Theoretical background

Figure 1 shows a schematic diagram of the FPM scenario wave vectors k_i ($i=1, 2, 3$), displaying the input pump beams ($\omega_1=\omega_2$), and the SHG beam (ω_3) inside the isotropic crystal. Input and output coupling occur through the slanted faces of the monolithic isotropic crystal.

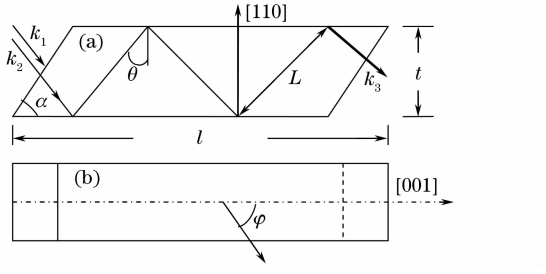

Fig. 1　Diagram of the FPM configuration. (a) Side view and (b) top view of the configuration.

In the nonresonant FPM scenario, the conditions of photo energy and momentum conversion of SHG also require that $2\omega_1=\omega_3$ and $\Delta k=2k_1-k_3=\pi/\Lambda_c$. There is one additional condition that must be satisfied[15]:

$$\Delta\phi=\Delta kL+\Delta\phi_F+\delta\phi-2n\pi=0, \qquad (1)$$

where n is an integer number, $L=t/\cos\theta=(2N+1)\Lambda_c$ is the zigzag length, t is the thickness of the crystal, N is the number of bounces, $N=\mathrm{EP}\left[1+\frac{l-t/\tan\theta}{t\tan\theta}\right]$ (EP[] means to get the integer port), and Λ_c is the periodical length given by the coherence length. The total Fresnel phase shift $\Delta\phi_F$ is used to compensate any phase shift in isotropic materials. The total phase shift $\Delta\phi$ among the interaction waves is the sum of the dispersion phase mismatch Δk, the relative Fresnel phase shift $\Delta\phi_F$ at the crystal-air interface, and the additional phase mismatch $\delta\phi$. The total Fresnel phase shift is

$$\Delta\phi_F=\phi_F^3-\phi_F^1-\phi_F^2, \qquad (2)$$

where $\phi_F^i=-2\arctan\left\{\frac{[(1-q)+qn_i^2]\sqrt{n_i^2\sin^2\theta-1}}{n_i\cos\theta}\right\}$ is Fresnel phase shift, and if the beam is p polarization, $q=1$, or else $q=0$ and $i=1, 2, 3$. The total internal reflection angle θ must be higher than the Descartes-Snell angle θ_c, $\sin\theta_c=1/n_{THz}$, as shown in Fig. 1. The additional phase shift $\delta\phi$ depends on the sign of the effective nonlinear coefficient: if the sign of the effective nonlinear coefficient changes at reflection, $\delta\phi=\pi$; if not, $\delta\phi=0$. In lossless case, the output intensity of SHG beam is given by[15]

$$I_3^{out}=\frac{Z_0\omega_3^2}{2c^2}\frac{(Nd_{eff})^2}{n_1^2n_3}\times\left[\frac{\sin(\Delta kL/2)}{\Delta k/2}\right]^2\left[\frac{\sin(N\Delta\phi/2)}{N\sin(\Delta\phi/2)}\right]^2I_1^2, \qquad (3)$$

where Z_0 is the vacuum impedance ($Z_0=377\Omega$), c is the speed of light, d_{eff} is the effective nonlinear coefficient, n_i ($i=1,3$) is the refractive index of pump beam and SHG beam, respectively, and I_i ($i=1,3$) displays the input intensity of pump beam and output intensity of SHG beam, respectively.

In this paper, the experimental model is based on the experiment reported in Ref. [11]. In simulation, the following parameters are taken: $\lambda_1=\lambda_2=3\sim6$ μm, the thickness of crystal t is equal to 360 μm for ZnSe crystal, and 400 μm for GaP crystal.

We also take the Snell equations of ZnSe and GaP crystals, which are researched by Li *et al.*[16,17]. The optical refractive index of GaAs crystal can be obtained from

$$n_j^2=1+\frac{4.2980149\lambda_j^2}{\lambda_j^2-(0.19206300)^2}+\frac{0.62776557\lambda_j^2}{\lambda_j^2-(0.37878260)^2}+\frac{2.8955633\lambda_j^2}{\lambda_j^2-(46.994595)^2}, \quad j=1, 2, 3. \qquad (4)$$

The optical refractive index of GaP crystal can be obtained by

$$n_j^2=2.680+\frac{6.40\lambda_j^2}{\lambda_j^2-0.0903279}, \ j=1,2,3. \qquad (5)$$

Because of eight different polarization combinations of the three waves, eight different polarization configurations are investigated on substituting Eqs. (4) and (5) into Eq. (1). Careful calculation shows that for given pump waves, only spp and pss configuration can provide QPM in ZnSe and GaP crystals, as shown in Fig. 2. In the case of $\lambda_1=\lambda_2=3.4$ μm, when $\theta=32.5°$ for nonresonant FPM ZnSe crystal in pss configuration, the condition of Eq. (1) can be satisfied, i.e., $\Delta\phi=2\pi$ with $\lambda_3=1.7$ μm and the condition of Eq. (1) also can be satisfied with $\theta=30.5°$ for nonresonant FPM ZnSe crystal in spp configuration, as shown in Fig. 2(a). The similar situation of nonresonant FPM GaP crystal is shown in Fig. 2(b). In the case of $\lambda_1=\lambda_2=3.4$ μm, when $\theta=33.1°$ in pss configuration, the condition of Eq. (1) can be satisfied, and it also can be satisfied with $\theta=20.7°$ in spp configuration.

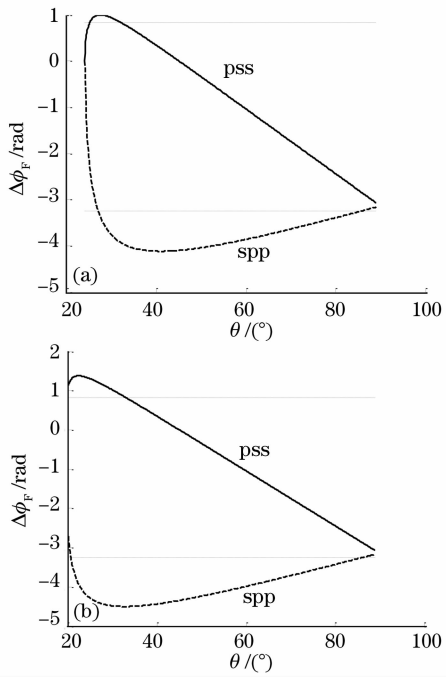

Fig. 2 Fresnel phase shift $\Delta\phi_F(3.4+3.4 \rightarrow 1.7\ \mu m)$ at total reflection interface both in FPM (a) ZnSe and (b) GaP crystal versus θ.

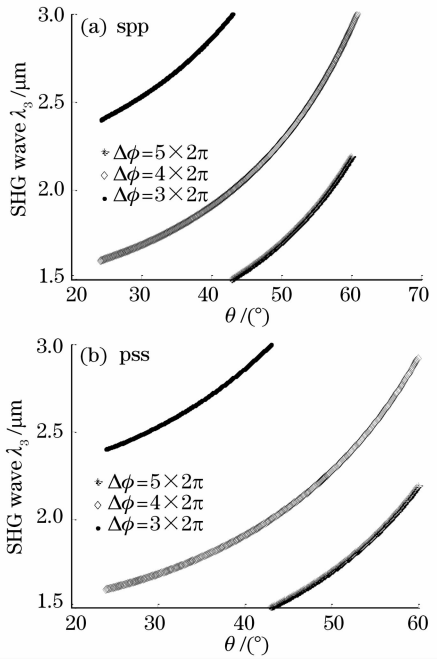

Fig. 3 Tuning range of λ_3 in nonresonant FPM ZnSe crystal versus θ under (a) spp and (b) pss polarization configurations, respectively.

3 Theoretical analysis of tuning characteristics

3.1 Angle tuning characteristics

Firstly, we analyze the angle tuning characteristics with $\Delta\phi = 2n\pi$ under spp and pss polarization configurations in nonresonant FPM ZnSe crystal. The angle tuning curve under different polarization configurations can be obtained by substituting Eqs. (2) and (4) into Eq. (1), as shown in Fig. 3.

Figure 3(a) shows that under spp configuration, when θ tunes from 24.05° to 60.9° with $\Delta\phi = 4\times2\pi$, the tuning range of SHG wave $\lambda_3 = 1.601 \sim 3\ \mu m$ is obtained. When the total phase shifts are $\Delta\phi = 3\times2\pi$ and $5\times2\pi$, the corresponding tuning ranges of SHG wave are $2.398 \sim 3\ \mu m$ and $1.5 \sim 2.192\ \mu m$ with $\theta = 24.2° \sim 43.1°$ and $42.19° \sim 60°$, respectively. In pss configuration, when the total phase shifts are $\Delta\phi = 3\times2\pi$, $4\times2\pi$ and $5\times2\pi$, the tuning ranges of θ and pump wave are $24.1°\sim43.1°$, $24°\sim60°$, $43°\sim60°$, $2.404 \sim 2.999\ \mu m$, $1.603 \sim 2.919\ \mu m$ and $1.502 \sim 2.192\ \mu m$, respectively, as shown in Fig. 3(b). Our calculation shows that when $\Delta\phi = 4\times2\pi$ and $\lambda_1 = \lambda_2 = 3.4\ \mu m$, θ equals 30.5° in spp configuration. There is a derivation between our calculation result and the reported experimental result[18]. One explanation of the discrepancy is based on the fact that Eq. (4) does not fit to refractive index of ZnSe crystal reported in Ref. [18]. Figures 3 (a) and (b) also show that, compared with these in pss configuration, the tuning range of SHG wave λ_3 is larger in spp configuration, and the angle tuning range is similar in different configurations. This means that spp configuration of ZnSe crystal is benefit to generate widely tunable SHG mid-infrared radiation in the experiment.

The angle tuning characteristics of nonresonant FPM GaP crystal under spp and pss configurations are also numerically analyzed, as shown in Fig. 4. When the condition of nonresonant FPM $\Delta\phi = 5\times2\pi$ is satisfied with $\theta = 24° \sim 57°$, the tuning range of SHG wave is $1.804 \sim 2.992\ \mu m$ in spp configuration and $1.806 \sim 2.994\ \mu m$ in pps configuration, respectively. When $\Delta\phi = 4\times2\pi$, the tuning range of SHG wave is $1.999 \sim 2.996\ \mu m$ and $2.244 \sim 3\ \mu m$ in spp and pss configurations, respectively. In this case, θ is in the range of $24°\sim52.7°$. The tuning range of SHG wave is $2.004 \sim 2.998\ \mu m$ and $2.246 \sim 2.998\ \mu m$ with $\Delta\phi = 3\times2\pi$ in the spp and pss configurations, where the same tuning range of θ is $24°\sim47.1°$. The simulation shows that the tuning ranges of SHG wave are almost the same with identic angle tuning range under different polarization configurations in nonresonant FPM GaP crystal.

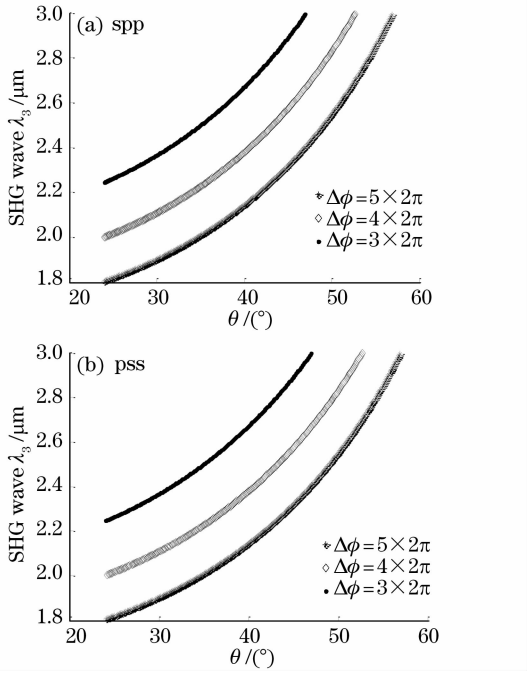

Fig. 4　Tuning range of λ_3 in nonresonant FPM GaP crystal versus θ under (a) spp and (b) pss polarization configurations, respectively.

3.2　Angular acceptance of SHG

When the condition of nonresonant FPM is satisfied, i.e., as Eqs. (1) and (3) show $\Delta\phi = 2n\pi$, the value of output signal intensity will be the maximum. It means that the signal intensity is determined primarily by the factor $[\sin(N\Delta\phi/2)/N\sin(\Delta\phi/2)]^2$ in Eq. (3). In the ideal assumption, this factor satisfies the condition of $\sin(N\Delta\phi/2) = 4/\pi^2$, i.e., $N\Delta\phi = 0.5 = 0.1592\pi$, to find the FWHM acceptance bandwidth for θ. In this case, $\Delta\phi$ as a function of θ is extended in a Taylor series about the value of θ_0 which achieves the condition of nonresonant FPM:

$$\Delta\phi(\theta) = (\theta-\theta_0)\left.\frac{\partial\Delta\phi}{\partial\theta}\right|_{\theta=\theta_0} + \left|\frac{1}{2}(\theta-\theta_0)^2\left.\frac{\partial^2\Delta\phi}{\partial\theta^2}\right|_{\theta=\theta_0} + \cdots = 0.1592\pi/N. \quad (6)$$

When the higher order terms of Eq. (6) is neglected, and only the influence of the first-order terms is considered, the FWHM acceptance bandwidth of θ is

$$\delta\theta = 2|\theta-\theta_0| \approx \frac{0.3184\pi}{N}\left|\left.\frac{\partial\Delta\phi}{\partial\theta}\right|_{\theta=\theta_0}\right|^{-1}. \quad (7)$$

In the case of $\lambda_1 = \lambda_2 = 3 \sim 6$ μm, Fig. 5 shows the FWHM acceptance bandwidth θ under different polarization configurations as a function of θ for nonresonant FPM ZnSe and GaP crystals. In nonresonant FPM ZnSe crystal under spp and pss configurations, the maximum FWHM acceptance bandwidths are always lower than 2.5 mrad, as shown in Figs. 5 (a) and (b). When $\theta = 24^\circ$ in the case of $\Delta\phi = 4\times2\pi$, the FWHM acceptance bandwidth of θ is 1.704 mrad, and the FWHM acceptance bandwidth of θ is equal to 0.37 mrad when $\theta = 60.9^\circ$ in spp configuration [Fig. 5(a)]. Figure 5(b) shows that in pss configuration with $\Delta\phi = 4\times2\pi$, the FWHM acceptance bandwidth of θ is 1.45 mrad with $\theta = 24^\circ$, and the FWHM

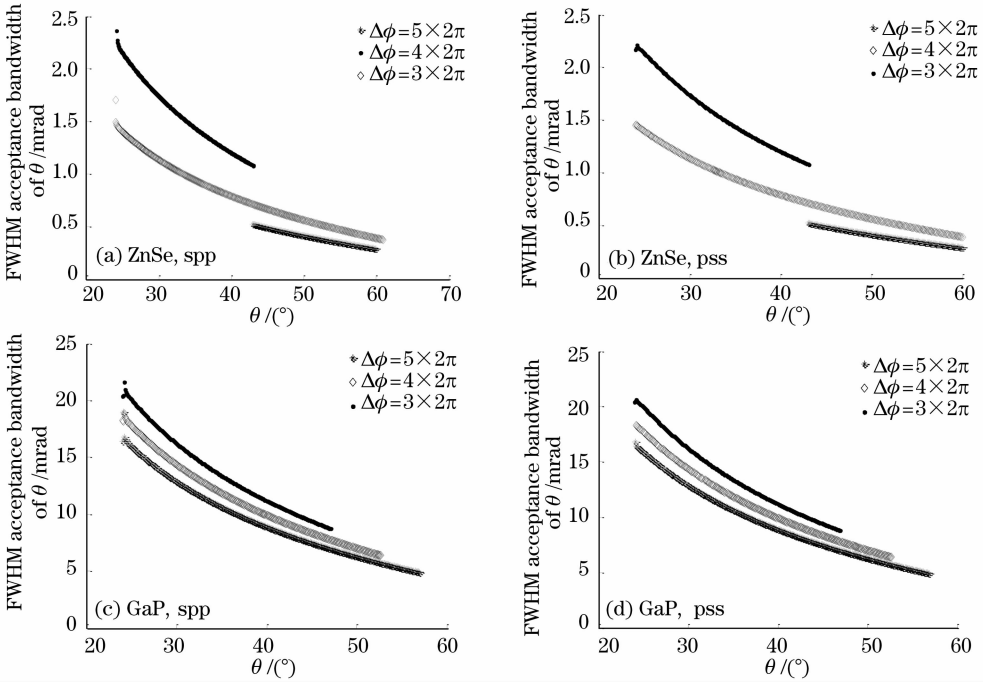

Fig. 5　FWHM acceptance bandwidth of θ in ZnSe and GaP crystals under (a),(c) spp and (b),(d) pss configurations, respectively.

acceptance bandwidth of θ is equal to 0.37 mrad when $\theta = 60.9^\circ$. The calculation shows that under different configurations, the FWHM acceptance bandwidth decreases with the increase of θ. Meanwhile, because of the small FWHM acceptance bandwidth of θ under different polarizations in ZnSe crystal, the path adjustment is difficult in the experiment.

In nonresonant FPM GaP crystal, larger FWHM acceptance bandwidth of θ is obtained, as shown in Figs. 5(c) and (d). In the case of $\Delta\phi = 5 \times 2\pi$, the FWHM acceptance bandwidth is equal to 16.77 mrad when $\theta = 24^\circ$, and $\delta\theta = 4.9$ mrad with $\theta = 57^\circ$ in spp configuration [Fig. 5(c)]. Figure 5(d) shows that $\delta\theta = 16.8$ mrad with $\theta = 24^\circ$, and $\delta\theta = 4.9$ mrad with $\theta = 57^\circ$ in spp configuration. The simulation shows that the FWHM acceptance bandwidth of θ is almost the same under different polarization configurations in GaP crystal. Comparing with the FWHM acceptance bandwidth of θ in ZnSe crystal, GaP crystal has a larger FWHM acceptance bandwidth of θ under different configurations, which will give convenience to adjusting path in the experiment.

3.3 Effective nonlinear coefficient d_{eff}

According to Eq. (3), higher effective nonlinear coefficient in a given polarization configuration is benefit to obtain higher output idler beam intensity for a given set of pump wave and SHG wave. Here we calculate the angle tuning characteristics of effective nonlinear coefficient of ZnSe and GaP crystals in the spp and pss configurations. In spp configuration, the nonlinear coefficient d_{eff} is described as[7]

$$d_{\mathrm{spp}} = d_{14}[3(\cos\theta\cos\phi)^2 + 1 - 2\cos^2\theta]\sin\phi. \quad (8)$$

The nonlinear coefficient d_{eff} in pss configuration is described as[7]

$$d_{\mathrm{pss}} = \frac{1}{4}d_{14}(\cos\phi + 3\cos 3\phi)\cos\theta, \quad (9)$$

where ϕ is the angle between the plane of incidence and [001] axis of the crystal, $d_{14} = 40$ pm/V[19] for ZnSe crystal and $d_{14} = 20$ pm/V[7] for GaP crystal, respectively. Calculation shows that, when ϕ is equal to 0° for the pss configuration and ϕ is equal to 30° for the spp configuration in both ZnSe and GaP crystals, the maximum value of effective nonlinear coefficient can be expected.

Figure 6 shows the influence of θ on the effective nonlinear coefficient both in FPM ZnSe crystal and GaP crystal under different polarization configurations. The effective nonlinear coefficient d_{eff} decreases with the increase of θ under different polarization configurations. The falling speed of the effective nonlinear coefficient in spp configuration is lower than the one in pss configuration. As shown in Fig. 6(a), when θ is less than 57.4°, the value of effective nonlinear coefficient in spp configuration is less than that in the pss configuration for FPM ZnSe crystal. However, when θ is equal to 90°, the effective nonlinear coefficient in pss configuration $d_{\mathrm{eff}} = 0$ pm/V, and the effective nonlinear coefficient $d_{\mathrm{eff}} = 20$ pm/V in spp configuration. The same situation of FPM GaP crystal is also shown in Fig. 6(b). Calculation shows that when the ZnSe crystal is used to be nonlinear crystal, spp configuration is benefit to obtain higher effective nonlinear coefficient with θ in the range of 24.05°～60.9°. GaP crystals in pss configuration will have higher effective nonlinear coefficient with $\theta < 57^\circ$.

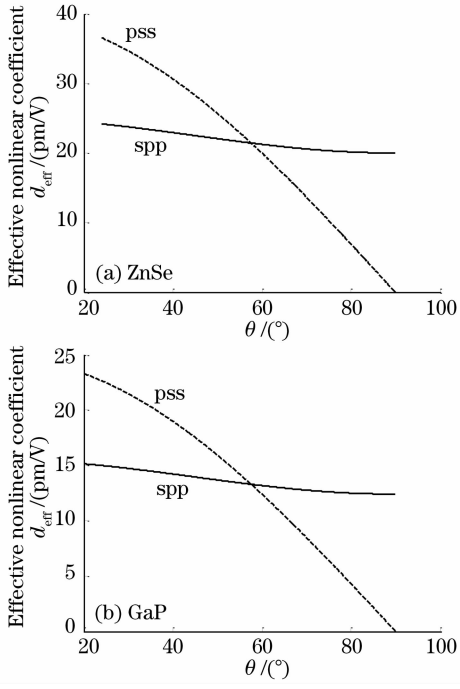

Fig. 6 Effective nonlinear coefficient versus θ under different polarization configurations for FPM (a) ZnSe crystal and (b) GaP crystal, respectively

4 Conclusion

We have theoretically investigated the tuning characteristics of tunable SHG mid-infrared radiation in FPM ZnSe and GaP crystals. Based on the technique of FPM, the parameters such as angle tuning characteristics, angular acceptance of SHG, and effective nonlinear coefficient of ZnSe and GaP

crystals are calculated and analyzed numerically. We find that, when the condition of nonresonant FPM $\Delta\phi = n \times 2\pi$ is satisfied in ZnSe crystal, the tuning range of SHG wave in spp configuration is larger than that in pss configuration. The FWHM acceptance bandwidth of θ in spp configuration is also similar to that in pss configuration. The calculation also shows that spp polarization configuration can be expected to have a better performance than pss configuration with a larger effective nonlinear coefficient, when the wavelength of SHG wave is less than 3 μm. When GaP crystal is used to be nonlinear crystal, the tuning ranges of θ and SHG wave λ_3, and the FWHM acceptance bandiwdth of θ are almost the same under different polarization configurations, respectively. Because the effective nonlinear coefficient of GaP crystal in pss configuration is larger than that in spp configuration with $\theta < 57°$, pss configuration is more suitable to generate SHG mid-infrared radiation in the experiment. Comparing with the FWHM acceptance bandwidth of θ in ZnSe crystal, GaP crystal has a larger FWHM acceptance bandwidth of θ under different configurations, which will offer convenience to adjusting path in the experiment. These theoretical calculations serve for the following tunable mid-infrared generation experiment in isotropic crystals as theoretical evidence and reference.

References

1 M. M. Fejer, G. A. Magel, D. H. Jundt *et al*.. Quasi-pahse-matched second harmonic generation: tuning and tolerances[J]. *IEEE J. Quantum Electron.*, 1992, **28**(11): 2631～2654

2 D. M. Ren, J. Z. Huang, Y. C. Qu *et al*.. Optical properties and CO_2 laser SHG with $HgGa_2S_4$ [J]. *Chin. Opt. Lett.*, 2003, **1**(10): 613～615

3 Huang Jinzhe, Ren Deming, Zhang Lili *et al*.. Experimental research on the second harmonic generation of TEA CO_2 laser in $AgGaSe_2$ crystal[J]. *Chinese J. Lasers*, 2004, **31**(5): 559～562
黄金哲，任德明，张莉莉 等. TEA CO_2 激光在 $AgGaSe_2$ 晶体中的倍频实验研究[J]. 中国激光，2004，**31**(5)：559～562

4 J. M. Auerhammer, E. R. Eliel. Frequency doubling of mid-infrared radiation in gallium selenide [J]. *Opt. Lett.*, 1996, **21**(11): 773～775

5 E. Lallier, M. Brevignon, J. Lehoux. Efficient second-harmonic generation of a CO_2 laser with a quasi-phase-matched GaAs crystal [J]. *Opt. Lett.*, 1998, **23**(19): 1511～1513

6 G. Olivie, P. Caumes, A. Bourqeade *et al*.. Spectral characterization of cascadingphenomena [C]. in Conference on Lasers and Electro-Optics 2001, 2001: 571～572

7 M. Barmentlo, G. W. Hooft, E. R. Elliel *et al*.. Sum-frequency generation with a free-electron laser: A study of gallium phosphide [J]. *Phys. Rev. A*, 1994, **50**(1): 14～17

8 M. Jin, Q. Cui, E. Mukhtar *et al*.. Second-harmonic generation measurement on ZnSe under high pressure [J]. *J. Phys.: Condens. Matter.*, 2002, **14**: 11037～11040

9 F. G. Parsons, E. Y. Chen, R. K. Chang. Dispersion of nonlinear optical susceptibilities in hexagonal Ⅱ-Ⅵ semiconductors[J]. *Phys. Rev. Lett.*, 1971, **27**(21): 1436～1439

10 S. Adachi. Model dielectric constant of GaP, GaAs, GaSb, InP, InAs, and InSb[J]. *Phys. Rev. B*, 1987, **35**(14): 7454～7463

11 C. H. Henry, J. J. Hopfield. Raman scattering by polaritons[J]. *Phys. Rev. Lett.*, 1965, **15**(25): 964～966

12 T. Tanabe, K. Suto, J. I. Nishizawa *et al*.. Frequency-tunable terahertz wave generation via excitation of phonon-polaritons in GaP[J]. *J. Phys. D: Appl. Phys.*, 2003, **36**: 953～957

13 Q. Wi, X. C. Zhang. 7 terahertz broadband GaP electro-optic sensor[J]. *Appl. Phys. Lett.*, 1997, **70**(14): 1784～1786

14 J. A. Amstrong, N. Bloembergen, J. Ducuing *et al*.. Interactions between light waves in a nonlinear dielectric[J]. *Phys. Rev.*, 1962, **127**(6): 1918～1939

15 R. Haidar, N. Forget, Ph. Kupecek *et al*.. Fresnel phase matching for three-wave mixing in isotropic semiconductors[J]. *J. Opt. Soc. Am. B*, 2004, **21**(8): 1522～1534

16 H. H. Li. Refractive index of ZnS, ZnSe, and ZnTe and its wavelength and temperature derivatives[J]. *J. Phys. Chem. Ref. Data*, 1984, **13**(1): 103～150

17 D. C. Yin, Y. Inatomi. Measurement of refractive index of GaP crystal over a large temperature range using interferometry[J]. *Crys. Res. Technol.*, 2000, **35**(2): 211～228

18 H. Komine, W. H. Long, Jr. J. W. Tully *et al*.. Stappaerts, quasi-phase-match second-harmonic generation by use of a total-internal-reflection phase shift in gallium arsenide and zinc selenide plates[J]. *Opt. Lett.*, 1998, **23**(9): 661～663

19 J. P. Caumes, L. Videau, C. Rouyer *et al*.. Kerr-like nonlinearity induced via Terahertz generation and the electro-optical effect in zinc blende crystals[J]. *Phys. Rev. Lett.*, 2002, **89**(4): 047401